reactions $BrO_3^- + BrO^- \rightleftarrows 2BrO_2^-$ in strongly alkaline solution and on an estimate[35] of 0.01 for the acid ionization constant of $HBrO_2$. Such constants for $HClO_2$ and HNO_2 are[24] 1.1×10^{-2} and 4.5×10^{-4}, respectively. If the estimate for $HBrO_2$ were reduced to 0.001, $E_b°$ would decrease 0.03 V.

The value for $E_a°$ is derived from observations[23,36] that permitted an estimate[6] of the equilibrium constant for $BrO_3^- + HBrO_2 + H^+ \rightleftarrows 2BrO_2\cdot + H_2O$. Any change in $E_b°$ would change $E_a°$ in the same direction but by only half as much.

Metal-Ion Catalysts. Reduction potentials are not well-defined for the strongly oxidizing substitution-labile ions. Latimer[24] quotes about 1.5 V for Mn(III) and 1.44 V for Ce(IV) in 1 M sulfuric acid. The substitution-inert catalysts are not as strong oxidants. Reported reduction potentials are 1.06 V[24] for $Fe(phen)_3^{3+}$ and 1.29 V[37] for $Ru(bpy)_3^{3+}$.

Aromatic Compounds. The potentials in Figure 3 for $HArO_2$, $HAr(OH)O\cdot$, and $HAr(OH)_2$ are those for the *p*-benzoquinone system. Those potentials are known to four significant figures;[38] potentials for other quinones in class ii are probably sufficiently similar for the purposes of this paper.

Oxalic Acid. Treatment of the oxalic acid examples of classes iii and iv requires potentials for half-reactions c and d. Data from

$$2CO_2 + 2H^+ + 2e^- = H_2C_2O_4 \quad (c)$$

$$CO_2 + \cdot CO_2^- + 2H^+ + e^- = H_2C_2O_4 \quad (d)$$

Latimer[24] indicate $E_c° = -0.39$ V. The facile oxidation of oxalate by manganese(III)[38] demonstrates that $E_d°$ is certainly less than 1.5 V, but no firm estimate is possible without information on the free energy of formation of $\cdot CO_2^-$. No effort has been made to illustrate this system in Figure 3.

Other Aliphatic Paired-Electron Compounds. Reduction potentials involving Q=O, HQOH, and QH_2 were calculated by use of the group additivities of Benson.[39] Such calculations should be valid to about 0.1 V in the gas phase. Differences in solvation will make the uncertainty greater in Figure 3 but will not alter the mechanistic conclusions.

Other Organic Radicals. Reactions of classes i, iii, and v involve one-equivalent oxidations of the species QH_2 and HQOH. If these are designated SH, entries in Figure 3 are derived from considering half-reactions e-g. If D's are bond dissociation enthalpies in

$$S\cdot(aq) + H^+(aq) + e^- = SH(aq) \quad (e)$$

$$H\cdot(g) + H^+(aq) + e^- = H_2(g) \quad (f)$$

$$S\cdot(g) + H_2(g) = SH(g) + H\cdot(g) \quad (g)$$

kcal/mol, the free-energy change in (g) can be approximated by (E1). If SH and S· have almost equal free energies of solvation,

$$\Delta G_g° \approx \Delta H_g° = D(H\text{-}H) - D(S\text{-}H) \quad (E1)$$

we obtain (E2). Data from Latimer[24] give $E_f° = 2.11$ V. Ta-

$$E_e° = E_f° - \frac{D(H\text{-}H) - D(S\text{-}H)}{23.0} \quad (E2)$$

bulations by Benson and O'Neal[40] suggest that for malonic acid (QH_2) D(S-H) should be about 88 kcal/mol and then $E_e° = 1.4$ V. For HQOH, D(S-H) should be about 84 kcal/mol and then $E_e° = 1.2$ V. These estimates are shown in Figure 3; they are more uncertain than the other values in the figure but probably no more than a few tenths of a volt. The qualitative mechanistic conclusions remain valid.

(34) Lee, C. L.; Lister, M. W. *Can. J. Chem.* **1971**, *49*, 2822.
(35) Pauling, L. "General Chemistry", 3rd ed.; W. H. Freeman: San Francisco, Calif., 1970; p 501.
(36) Betts, R. H.; MacKenzie, A. N. *Can. J. Chem.* **1951**, *29*, 655.
(37) Bock, C. R.; Meyer, T. J.; Whitten, D. G. *J. Am. Chem. Soc.* **1974**, *96*, 4710.
(38) Adler, S. J.; Noyes, R. M. *J. Am. Chem. Soc.* **1955**, *77*, 2036.
(39) Benson, S. W. "Thermochemical Kinetics", 2nd ed.; Wiley: New York, 1976.
(40) O'Neal, H. E.; Benson, S. W. "Free Radicals"; Kochi, J. K., Ed.; Wiley: New York, 1973; Vol. II, p 285.

Diffusional Charge Transport through Ultrathin Films of Radiofrequency Plasma Polymerized Vinylferrocene at Low Temperature

P. Daum, J. R. Lenhard, D. Rolison, and Royce W. Murray*

Contribution from the Kenan Laboratories of Chemistry, University of North Carolina, Chapel Hill, North Carolina 27514. *Received December 26, 1979*

Abstract: In room-temperature butyronitrile, films of plasma polymerized vinylferrocene on Pt electrodes, which contain 7-10 $\times 10^{-9}$ mol/cm^2 of ferrocene sites, undergo rapid exchange of electrons with the Pt electrode. At low temperature (-50 to -85 °C), the transport of electrochemical charge through the polymer film is controlled by diffusion according to Fick's law under infinite and finite boundary conditions depending on time and temperature. Activation energies and entropies for the charge-diffusion process are approximately 3.7 kcal/mol and -32 cal/(mol deg), respectively. Charge diffusion is interpreted as controlled by the cooperative motions of polymer chains required for site-site collisions and counterion transport. The electron self-exchange rate between ferrocene and ferricenium sites is diffusion controlled and approximately 10^2 L/(mol s).

Considerable attention has been given recently to the preparation and properties of thin films of polymeric materials bonded to or coated on metal and semiconductor electrodes.[1-9] In many cases the polymer films contain, or are later modified to contain, electrochemically reactive groupings. These groupings can be

(1) (a) Miller, L. L.; Van De Mark, M. R. *J. Electroanal. Chem.* **1978**, *88*, 437; (b) *J. Am. Chem. Soc.* **1978**, *100*, 639. (c) Van De Mark, M. R.; Miller, L. L. *Ibid.* **1978**, *100*, 3223. (d) Kerr, J. B.; Miller, L. L. *J. Electroanal. Chem.* **1979**, *101*, 263.
(2) Kaufman, F. B.; Engler, E. M. *J. Am. Chem. Soc.* **1979**, *101*, 547.
(3) Döblhofer, K.; Nolte, D.; Ulstrup, J. *Ber Bunsenges. Phys. Chem.* **1978**, *82*, 403.
(4) (a) Wrighton, M. S.; Austin, R. G.; Bocarsly, A. B.; Bolts, J. M.; Haas, O.; Legg, K. D.; Nadjo, L.; Palazzotto, M. C. *J. Electroanal. Chem.* **1978**, *87*, 429; (b) *J. Am. Chem. Soc.* **1978**, *100*, 1602. (c) Bolts, J. M.; Wrighton, M. S. *Ibid.* **1978**, *100*, 5257. (d) Bolts, J. M.; Bocarsly, A. B.; Palazzotto, M. C.; Walton, E. G.; Lewis, N. S.; Wrighton, M. S. *Ibid.* **1979**, *101*, 1378.

0002-7863/80/1502-4649$01.00/0

oxidized and reduced by the electrode even though the films in some cases contain the equivalent of several hundred monolayers of redox sites. Redox polymer coated electrodes show promise in electrochromic,[2] electrocatalytic[1d,4d] and antiphotocorrosion[4c,4d] experiments. Key to success in such applications, ultimately, is the rate at which electrochemical charge can be made to propagate through the redox polymer film. Quantitative measurements of charge-transport rates are therefore of interest.

The mechanism(s) controlling the migration of electrochemical charge through redox polymers are also of interest. For a pyrazoline redox polymer, it was proposed[2] that electron transfer between interacting pyrazoline sites is the controlling process in the solvent swollen polymer. Although qualitatively reasonable, this proposal was not supported by any quantitative evidence.

Oxidation or reduction of fixed sites introduces charged sites into a polymer film and so requires, for charge neutrality, ingress of counterions from the contacting electrolyte solution, and, by the Donnan relation, egress of coions. Thus, while electron hopping may be a *mechanism* for *electron transport*, it is possible that either ion motions or electron hopping can constitute the *rate-controlling* event for overall *charge transport*.

In its simplest form, charge-transport control by either electron hopping or ion transport in a redox polymer film undergoing electrolysis should follow Fick's diffusion law[10] and be identifiable by comparing transient electrochemical data to Fick's law based transport relations. However, electrochemical charging of a redox polymer film involves several factors which may cause Fickian equations to fail: (i) ion transport control (A strong ion or solvent population disequilibrium, as is well-known in ion-exchange resin transport[11] and in poorly swollen glassy polymers,[12,13] can yield apparent non-Fickian behavior, because ion diffusion constants vary over the gradients of ion activity coefficients, solvent content and osmotic flow, polymer lattice expansion, and electrostatic ion-site effects which accompany the disequilibrium.), (ii) noncontinuum (In the case of films a small number of monolayers thick, the number of electron hops may be too small to approximate the continuum on which Fick's law is based.), (iii) film discontinuities (Little is known about the physical topology of redox polymer films spread on electrodes. In films containing discontinuities such as filamented sections, charge flow from a relatively large volume of reacting polymer may be controlled by a small number of discontinuities which act as barriers.), (iv) concentration polarization (Since change in the internal ion concentration in the polymer can be large, ions in the solution contacting the polymer film may become concentration polarized.), and (v) film resistance (The charge transport resistance of the polymer film is an ohmic resistance *uncompensated* by the use of three electrode cells, which may cause loss of potential control particularly in potential *sweep* experiments.). The opportunities for non-Fickian effects are thus sufficiently great that examples of Fick's law charge-transport behavior in redox polymer films are of current importance.

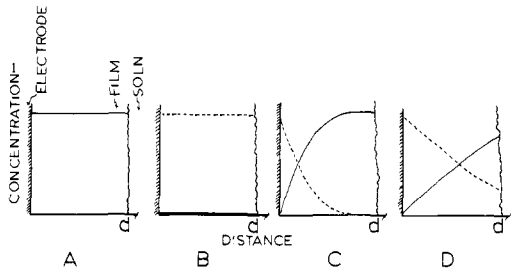

Figure 1. Schematic representation of concentration–distance profiles of concentrations (C) of ferrocene (—) and ferricenium (- - -) states at an arbitrary time after application of a positive-going potential step to a film of I initially in the ferrocene state. The final potential is selected so that at the electrode polymer interface [ferricenium]/[ferrocene] >100: curve A, initial state of film; curve B, very fast charge transport; curve C, very slow charge transport, semiinfinite diffusion; curve D, intermediate charge-transport rate, finite diffusion. d = film thickness in cm, x = distance from metal electrode.

An electrode coated with a redox polymer film of uniform composition and thickness d which does exhibit diffusive charge transport may do so at a rate fast, slow, or intermediate with respect to the experimental time scale. If the charge transport rate is significantly faster than the experimental time scale, the oxidized/reduced site concentration ratio Γ_O/Γ_R will be both uniform throughout the film and in thermodynamic equilibrium with the applied electrode potential (Figure 1B). Cyclic voltammetric current–potential peaks will have a symmetrical shape in this case. If on the other hand the diffusion constant D for charge transport is very small, such that during the experiment the distance of charge transport $l \approx 2(Dt)^{1/2} < d$ (Figure 1C), data taken with cyclic voltammetry and potential step chronoamperometry will quantitatively be the same as when reactants freely diffuse to the electrode from an infinite volume of solution. In this case, data will obey the Randles–Sevcik[14] and Cottrell[15] equations, respectively. At an intermediate charge-transport rate, the diffusion gradients will impinge on the outer boundary of the polymer film (Figure 1D), and Fick's Law relations based on a *finite* volume of polymer reactant will be obeyed. Such relations are the same as those in thin layer electrochemistry[17] except that the polymer film is ca. 10^3 thinner than the usual thin layer electrochemical cell.

We became interested in this problem during studies of films of polymerized vinylferrocene deposited on Pt and glassy carbon electrodes from radiofrequency Ar plasmas.[6a,e,18] Apparent Fick's Law characteristics emerged in experiments using nitrile solvents.[18] Although the chemical composition of films of plasma-polymerized vinylferrocene, I, is more complex than that of poly(vinylferrocene), II, as is typical of plasma generated polymers,[19] the electrochemical properties of I are nonetheless qualitatively, in reversible potential, solvent dependence, and wave shape effects, similar to those observed for films of II in our laboratories.[20] The plasma film has the advantage of comparative smoothness and is easy to prepare.

We have found that films of plasma-polymerized vinylferrocene can be made to exhibit the three regimes of charge-transport behavior by manipulation of butyronitrile solvent temperature over a 100 °C span. We demonstrate this here and show that Fick's Law is quantitatively obeyed in the slower charge transport re-

(5) (a) Merz, A.; Bard, A. J. *J. Am. Chem. Soc.* **1978**, *100*, 3222. (b) Itaya, K.; Bard, A. J. *Anal. Chem.* **1978**, *50*, 1487.

(6) (a) Nowak, R.; Schultz, F. A.; Umaña, M.; Abruña, H.; Murray, R. W. *J. Electroanal. Chem.* **1978**, *94*, 219. (b) Murray, R. W. "Symposium on Silylated Surfaces", Midland Macromolecular Monograph, Gordon and Bruch, in press. (c) Lenhard, J. R.; Murray, R. W. *J. Am. Chem. Soc.* **1978**, *100*, 7870. (d) Abruña, H.; Meyer, T. J.; Murray, R. W. *Inorg. Chem.*, **1979**, *18*, 3233. (e) Daum, P.; Murray, R. W. *J. Electroanal. Chem.* **1979**, *103*, 289.

(7) (a) Oyama, N.; Anson, F. C. *J. Am. Chem. Soc.* **1979**, *101*, 739; (b) *Ibid.* **1979**, *101*, 3450.

(8) Fischer, A. B.; Wrighton, M. S.; Umaña, M.; Murray, R. W. *J. Am. Chem. Soc.* **1979**, *101*, 3442.

(9) Kaufman, F. B.; Schroeder, A. H.; Engler, E. M.; Kramer, S. R.; Chambers, J. Q. *J. Am. Chem. Soc.* **1980**, *102*, 483.

(10) $\delta C/\delta t = D(\delta^2 C/\delta x^2)$, where D is the charge transport diffusion constant and C is the concentration of redox sites.

(11) Meares, P. In "Diffusion in Polymers"; Crank, J., Park, G. S., Eds.; Academic Press: New York, 1968; p 373.

(12) Park, G. S. In "Diffusion in Polymers"; Crank, J., Park, G. S., Eds.; Academic Press: New York, 1968; "The Glassy State and Slow Process Anomalies".

(13) Rebenfeld, L.; Makarewicz, P. J.; Weigmann, H.-D.; Wilkes, J. L. *J. Macromol. Sci., Rev. Macromol. Chem.* **1976**, *C15*, 279.

(14) Reversible Randles–Sevcik equation, $i_p = 2.72 \times 10^5 n^{3/2} A D^{1/2} C v^{1/2}$, ref 16, p 119.

(15) Cottrell equation $i = nFAD^{1/2}C/\pi^{1/2}t^{1/2}$, ref 16, p 51.

(16) Delahay, P. "New Instrumental Methods in Electrochemistry"; Interscience: New York, 1954.

(17) Oglesby, D. M.; Omang, S. H.; Reilley, C. N. *Anal. Chem.* **1965**, *37*, 1312.

(18) Nowak, R. J.; Schultz, F. A.; Umana, M.; Lam, R.; Murray, R. W. *Anal. Chem.* **1980**, *52*, 315.

(19) Millard, M. In "Techniques and Applications of Plasma Chemistry"; Hollahan, J. R., Bell, A. T., Eds.; Wiley: New York, 1974, p 177.

(20) Daum, P.; Rolison, D.; Murray, R. W., unpublished results, 1979.

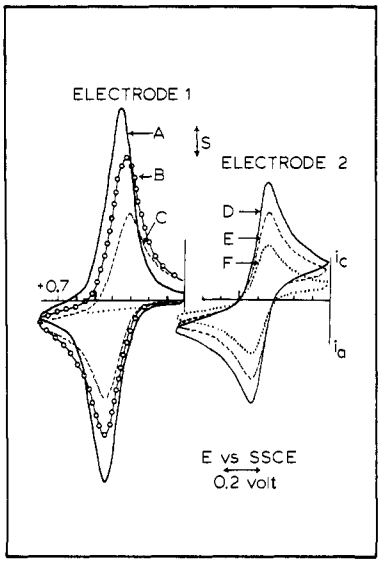

Figure 2. Cyclic voltammograms of I deposited on two different Pt electrodes, in 0.1 M Bu_4NClO_4/butyronitrile. Curves A–C recorded at +20, −53, and −72 °C, respectively, at 200 mV/s (S = 44.3 $\mu a/cm^2$); Curves D–F recorded at −70 °C at 50 mV/s (S = 8.8 $\mu a/cm^2$), 100 mV/s (S = 17.6 $\mu a/cm^2$), and 200 mV/s (S = 35.2 $\mu a/cm^2$), respectively. Coverage measured from charge above base line current, $\Gamma = 4.06 \times 10^{-9}$ mol/cm^2 (curve A), 3.33×10^{-9} (curve B), 2.08×10^{-9} (curve C). ΔE_p = 70, 110, 125, 85, 90, and 88 mV for curves A–F, respectively.

gimes. The activation energy and entropy for charge transport have been determined and are revealing as to the probable molecular nature of the charge-transport rate limitation.

Experimental Section

Radiofrequency Plasma Polymerization of Vinylferrocene. Details of the polymerization experiment are presented elsewhere.[6a,18] In the present study, films of I are prepared by using 1–3-min plasma reaction periods under conditions seeking a high rate of polymer film formation: plasma reactor geometry B[18] with a ca. 0.5-cm separation between the surface of the Pt electrode and the charge of solid vinylferrocene monomer and a substantially larger charge of the monomer than used earlier,[18] 75–100 mg of vinylferrocene powder spread over a ~10-cm^2 area. Elemental analysis of I harvested from reactor walls, which is hard and somewhat powdery, indicates the empirical formula of $FeC_{10}H_{11}O_{1.7}$, similar to the earlier determined composition. However, less degradation of ferrocene sites in the film has occurred due to the fast deposition rates employed; Fe $2p_{3/2}$ XPS shows a ferrocene band (708.7 eV) 5–10 times, more intense than the 711-eV peak which is a mixture of ferricenium and Fe(III) decay product attached to the polymer.[21] SEM of films of I at 1-μm resolution shows a rather smooth surface, with faint, rounded dimpling and no visible pores.[18]

Films of I deposited at high rates contain some low molecular weight fragments which are solubilized upon cyclic voltammetric scanning in acetonitrile or butyronitrile, as seen by a 2–5 times diminution of the ferrocene electrochemical wave between the first and second potential cycles. Several days aging in air diminishes this effect; aged films were used in this study. Thereafter, the film of I is quite durable, its electrochemistry when held in the ferrocenium state decaying with a typical half-life of 1–2 h. The cyclic voltammetric waves of films of II decay in a similar manner[20] except that a large first scan change in the wave is not seen.

Electrochemical Experiments. Procedure involved recording several cyclic voltammetric scans of the film at room temperature in 0.1 M Bu_4NClO_4/butyronitrile, cooling and equilibrating the electrochemical cell at the lowest attainable temperature to record desired cyclic voltammetric and potential step (0 to +0.7 V vs. SSCE) chronoamperometric current–time curves, and gradually warming the cell to obtain data at higher temperatures. Data taken during the cooling cycle were identical but less conveniently obtained.

The electrochemical apparatus was conventional and equipped with positive feedback compensation to deal with ohmic effects associated with low temperature experiments. Ohmic effects were actually modest by using a well-designed cell with a Luggin capillary junction to the reference electrode, and in test experiments were mostly compensatable by using the positive feedback approach. Minor effects remaining are probably due to internal resistance of the film of I itself. Other experiments with the same apparatus at comparable low temperatures and current densities with surface-immobilized molecules[22] have produced current–potential responses free from the wave tailing of Figure 2, as further evidence of the absence of ohmic artifacts.

Electrochemical potentials are measured relative to a room-temperature SSCE connected to the cell with a salt bridge and Luggin probe.

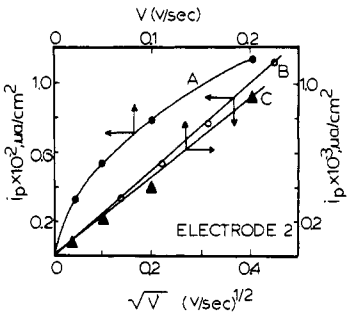

Figure 3. Cyclic voltammetric peak currents i_p plotted against potential scan rate v for surface Nernstian response[23] and $v^{1/2}$ for semiinfinite diffusion response[14]: curves A and B, −70 °C; curve C, 20 °C, electrode 2 of Figure 2.

Results and Discussion

A typical room-temperature cyclic voltammogram of a film of I on Pt in butyronitrile solvent is shown in Figure 2A. The anodic and cathodic current peaks are separated by small ΔE_{peak} (~40–50 mV usually) and are symmetrically shaped irrespective of scan rate over the range v = 0.005–0.2 V/s. Peak currents are proportional to potential scan rate[23] (Figure 3C), and the charge under the wave for ferrocene oxidation and rereduction is independent of v. These are all expected characteristics for fast charge transport through I as in Figure 1B.

The cyclic voltammetry of I distinctively changes at lowered temperature (Figure 2B,C). The current–potential wave grows a "tail", ΔE_{peak} becomes >50 mV, and the electrochemical wave becomes much smaller. As measured by charge above base line, the quantity of ferrocene oxidized in the low-temperature anodic wave of Figure 2C is only ca. 50% of that known to exist on this electrode from the (Figure 2A) room-temperature wave. The ferrocene sites are not exhaustively oxidized at low temperature, because the rate of charge transport is now slower than the experimental time scale. Figure 2D–F shows that as long as scan rate remains moderately fast, the tailing wave shape and ΔE_{peak} at low temperature are substantially unaffected by scan rate. Also, using 0.4 M Bu_4NClO_4 electrolyte in one low-temperature experiment caused no change in voltammetric behavior.

The temperature effects are completely reversible. Upon warming of either electrode of Figure 2 to room temperature, the originally symmetrical, larger current–potential pattern is quantitatively regenerated. Recooling repeats the data of Figure 2.

The low-temperature voltammograms of Figure 2 qualitatively resemble those of solution-dissolved reactants diffusing to the electrode, for which semiinfinite diffusion anticipates[14] a proportionality between peak current i_p and $v^{1/2}$. This proportionality is observed (Figure 3B), indicating that charge transport through I obeys Fick's Law at low temperature.

Potential step chronoamperometric experiments were carried out to more closely examine the charge diffusion behavior, with results shown in Figure 4. The i–$t^{-1/2}$ prediction of the semiinfinite diffusion-based Cottrell equation[15] is observed at sufficiently short time in the current–time decay. The linear region of the i–$t^{-1/2}$ plot is more extended at lower temperature. The fall-off of current indicates that at longer times the volume of polymer I cannot be taken as infinite and a finite diffusion boundary condition must be invoked. For a potential step experiment with a reactant

(21) Umana, M.; Rolison, D. R.; Nowak, R.; Daum, P.; Murray, R. W. *Surf. Sci.*, in press.

(22) Lenhard, J. R. Ph.D. Thesis, University of North Carolina, 1979.
(23) Lane, R. F.; Hubbard, A. T. *J. Phys. Chem.* **1973**, *77*, 1401.

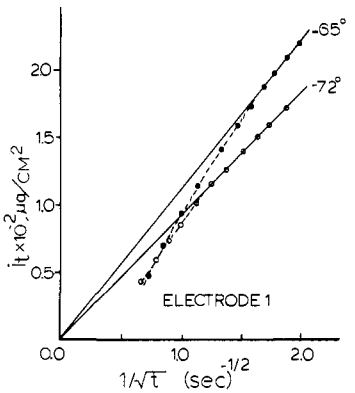

Figure 4. Chronoamperometric current–time data (● and ○) for a 4.06 × 10^{-9} mol/cm² film of I following potential step from 0 to +0.7 V vs. SSCE in 0.1 M Bu_4NClO_4/butyronitrile. Dashed lines are calculated by using eq 1 (see text). Electrode area is 0.113 cm².

Table I. Diffusion Constants and Energies for Charge Transport in Films of Plasma-Polymerized Vinylferrocene on Pt, in 0.1 M Bu_4NClO_4/Butyronitrile

electrode	T, °C	$10^9 \times D^{1/2}C$,[b] mol/(cm² s$^{1/2}$)	E_a,[c] cal/mol	$10^7 \times D_0^{1/2}C$,[c] mol/(cm² s$^{1/2}$)
1 ($\Gamma = 4.06 \times 10^{-9}$ mol/cm²)[a]	−52	2.71	3500	2.28
	−65	2.06		
	−72	1.66		
4 ($\Gamma = 1.1 \times 10^{-8}$ mol/cm²)[a]	−50	1.92	3900	1.06
	−60	1.58		
	−70	1.33		
	−80	1.03		
	−84	0.95		

[a] From room-temperature voltammograms. [b] From plots of chronoamperometric data, Figure 4. [c] From Figure 5.

solution of thickness d, the finite diffusion current–time relation is[17]

$$i = \frac{nFAD^{1/2}C}{\pi^{1/2}t^{1/2}}\left[\sum_{k=0}^{\infty}(-1)^k\left\{\exp\left(\frac{-k^2d^2}{Dt}\right) - \exp\left(\frac{-(k+1)^2d^2}{Dt}\right)\right\}\right] \quad (1)$$

For a comparison of eq 1 to the experiment, D and d are required, or more precisely, the ratio d^2/D is needed. The slope[15] of the linear (short time) region of the i–$t^{-1/2}$ plot provides the product $D^{1/2}C$, where D is the charge-transport diffusion constant and C is the concentration of ferrocene sites in I. Since the average $C = \Gamma/d$, and Γ is already known from the room-temperature result, d^2/D is obtainable as $(\Gamma/D^{1/2}C)^2$. By this means, the longer time current–time data for the experiments of Figure 4 were computed from eq 1. The theoretical prediction (dashed line) agrees exactly with the experimental points (Figure 4), confirming that in these experiments a transition occurs, with increasing time in the potential step experiment, from the semiinfinite diffusion condition of Figure 1C to the finite diffusion condition of Figure 1D. Similar results were obtained over a range of temperatures and the chronoamperometric data are given in Table I. The results assert that charge transport in films of I at low temperature quantitatively follows Fick's diffusion law.

Emergence of diffusion control in low-temperature electrochemistry of films of I is clearly a consequence of thermally slowing the charge transport kinetics, so slowing the rate of electrochemical oxidation of the film sufficiently should restore the equilibrium (Figure 1B) behavior observed at room temperature. Thus, at very slow scan rates, the low-temperature voltammetric peak for I is symmetrical (compare Figure 5A,B) and the quantity of ferrocene reacting increases to a value, $\Gamma = 4.6 \times 10^{-9}$ mol/cm², close to that measured (for this electrode) at room

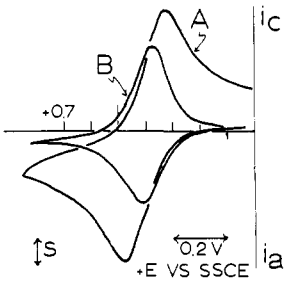

Figure 5. Cyclic voltammograms of I at −70 °C at 50 mV/s (curve A) and 1 mV/s (curve B) potential scan rates (electrode 3): curve A, S = 11.7 μa/cm², ΔE_p = 130 mV; curve B, S = 0.88 μa/cm², ΔE_p = 30 mV, $\Gamma = 4.6 \times 10^{-9}$ mol/cm².

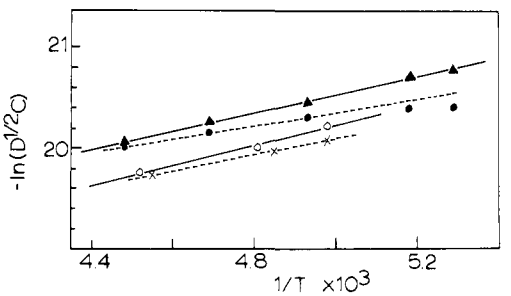

Figure 6. Arrhenius plot of diffusion coefficients obtained from chronoamperometric potential step (▲ and ○) and cyclic voltammetry (●, ×) experiments: electrode 1 (○ and ×) and electrode 4 (● and ▲).

temperature, 5.0×10^{-9} mol/cm². All of the ferrocene in the film can react if the low-temperature experiment is conducted slowly enough.

What is actually the diffusing entity during an anodic, ferrocene → ferricenium reaction in a film of plasma-polymerized vinylferrocene at low temperature? It obviously would be diffusing ferrocene if the electrode were naked Pt in contact with a solution of dissolved ferrocene. Ferrocene and ferricenium sites in the polymer film are mobile however only to the extent that polymer chains to which they are attached can undergo segmental motions of significant frequency and amplitude. If on the other hand we recognize that neighbor ferrocene and ferricenium sites can undergo electron-exchange reactions with one another, so that localized oxidation states migrate by electron hopping, we obtain a charge diffusion picture mathematically equivalent to freely diffusing ferrocene and ferricenium. The diffusants in the anodic reaction are *localized ferrocene states* (electrons) moving toward the electrode and *localized ferricenium states* moving away from the electrode. Figure 1C,D thus validly represents concentration–distance profiles of fixed ferrocene sites in the film at a given time during electrolysis. Diffusion of localized states would be accompanied by counterions migrating toward and coions migrating away from the electrode to maintain charge neutrality.

The picture of diffusing localized states does not specify whether the barriers for electron hopping or those for counterion (coion) motion control the rate of charge transport. If the barrier E_a is formulated as for thermally activated diffusion, expressing the diffusion constant in terms of the experimentally measured $D^{1/2}C$, we have

$$D^{1/2}C = D_0^{1/2}C \exp(-E_a/2RT) \quad (2)$$

Figure 6 shows that the experimental $D^{1/2}C$ values[24] depend on temperature in the expected way. Results from Figure 6 for E_a and $D_0^{1/2}C$ are given in Table I.

The concentration C of ferrocene sites in the film is not known accurately, but if we assume a ferrocene density of 0.5 g/cm³, $C \approx 2.4 \times 10^{-3}$ mol/cm³ and $D_0 = 10^{-8}$ and 2×10^{-9} for electrodes

(24) $D^{1/2}C$ was obtained from cyclic voltammetric i_p–$v^{1/2}$ plots (such as Figure 3) by using the Randles–Sevcik Equation[14] and from chronoamperometric i–$t^{1/2}$ plots discussed in connection with Figure 4.

1 and 4, respectively. The actual diffusion constants D in Table I range from 10^{-13} to 10^{-12} cm^2/s. Even a 10-fold uncertainty in C would not alter the fact that these diffusion constants and the D_0 preexponential are extraordinarily small.

The barrier E_a to localized state diffusion, ~3.7 kcal/mol, in these films in not especially distinctive in comparison to activation energies common for ions and molecules diffusing in solution and in ion-exchange resins[11,25-29] and for small molecules diffusing in neutral polymers, 2-8 kcal/mol. Ferrocene in acetonitrile[30] has for example E_a = 2.1 kcal/mol[24] and $D_{298} = 10^{-6}$ cm^2/s. Charge diffusion in I has (extrapolated) $D_{298} = 10^{-12}$–10^{-11} cm^2/s. This difference between the two kinds of ferrocene is mainly caused by D_0 rather than the activation energy term.

Diffusion in polymers is a complex topic and the preexponential factor D_0 has been formulated theoretically in several ways.[31] It is however not obvious that the diffusive combination of counterion and localized state migration envisioned here has a clear counterpart in the types of diffusion in the existing polymer literature. If we adopt, for simplicity, the Eyring formulation[25,31] for D_0

$$D_0 = e\lambda^2 \frac{kT}{h} \exp[\Delta S^*/R] \qquad (3)$$

where λ is diffusion jump distance and ΔS^* is entropy of activation, ΔS^* can be calculated by assuming that the number of jumps $d/\lambda = \Gamma/\Gamma_{monolayer}$, where $\Gamma_{monolayer} \approx 2 \times 10^{-10}$ mol/cm^2 for ferrocene. This assumption yields $D_0/\lambda^2 = (D_0^{1/2}C/\Gamma_{monolayer})^2$ from which at 200 K, $\Delta S^* = -32$ and -35 cal/(mol deg) for electrodes 1 and 4 of Table I, respectively. Thus, if represented as eq 3, the reason for the small value of D_0 and slow charge transport is a very large and negative entropy term. By this analysis, a charge-transport step requires an elastic and entropically ordering deformation of polymer chains in some volume or activation zone around the ferrocene and ferricenium sites between which charge transfer occurs. This is a reasonable result inasmuch as motion of the ferrocene and ferricenium sites into proper juxtaposition for electron transfer is certainly an ordering event and requires cooperative motion of the polymer backbone to which they are attached. Additionally, transport of the companion counterion (and solvent) requires expansion of the polymer lattice, reducing the mobility of polymer segments. Site mobility was in a previous case[2] judged dominant; we propose that for films of plasma-polymerized vinylferrocene, polymer lattice mobility is via eq 3 a better description of the charge diffusion-rate-controlling factor.

A possible alternative interpretation of the small D_0 preexponential invokes electron tunnelling between relatively immobile ferrocene and ferricenium sites separated by much larger distances than assumed above. Because this view does not assign implicit importance to the counterion motion and because entropic control of polymer motions has many precedents, we favor an interpretation based on molecular motions according to eq 3. Further tests of this possibility, however, seem warranted in future work.

It is of interest to estimate the rate of fruitful collison of ferrocene and ferricenium sites in the film required to support the measured rate of charge diffusion. Using $C = 2.4 \times 10^{-3}$ mol/cm^3 and $D = 4.9 \times 10^{-13}$ cm^2/s at −72 °C, simple collision rate theory[32] leads to $Z \sim 300$ s^{-1} (per site) or a period of ~3 ms between electron-transfer encounters for a given site. *This is also the maximum turnover rate at which ferrocene or ferricenium sites in these films can act as electron-transfer mediators in an electrocatalytic application where the substrate does not penetrate the film.* Finally, put in different units, this collision rate corresponds to a *diffusion-controlled electron-exchange rate* between ferrocene sites of $\sim 10^2$ L/(mol s). This is very slow compared to our usual concepts of diffusion-limited rates and is much slower than the measured[33] self-exchange rate for ferrocene dissolved in methanol at −75 °C, 8×10^6 L/(mol s). *This comparison accentuates the importance of the polymer framework in controlling electron self-exchange (i.e., electron hopping) between ferrocene and ferricenium sites in thin redox polymer films.* We are not aware of a diffusion-limited electron self-exchange rate smaller than 10^2 L/(mol s) having been previously detected.

Acknowledgments. This research was supported in part by a grant from the National Science Foundation. Professor Daum acknowledges sabbatical leave support from Northern Illinois University. This is part 21 of a series on Chemically Modified Electrodes.

(25) Bowers, R. C.; Murray, R. W. *Anal. Chem.* **1966**, *38*, 461.
(26) Helfferich, F. "Ion Exchange"; McGraw-Hill: New York, 1962.
(27) Wang, J. H.; Miller, S. *J. Am. Chem. Soc.* **1952**, *74*, 1611.
(28) Meares, P. *J. Am. Chem. Soc.* **1954**, *76*, 3415.
(29) Boyd, G. E.; Soldano, B. A. *J. Am. Chem. Soc.* **1953**, *75*, 6091, 6099.
(30) Van Duyne, R. P.; Reilley, C. N. *Anal. Chem.* **1972**, *44*, 142.
(31) MacGregor, R. "Diffusion and Sorption in Films and Fibers"; Academic Press: New York, 1974; Vol. 1, Chapter 15.
(32) Benson, S. W. "Foundations of Chemical Kinetics"; McGraw-Hill: New York, 1960; p 476.
(33) Stranks, D. R. *Discuss. Faraday Soc.* **1960**, *29*, 73.